If we only take in account the action of filter, it shows that the variances of phonton number fluctuation are much relative to propagation rate, distance between amplifiers, and bandwidth of the filter. High transmission rate, long repeat distance enlarge the energy jitters. The wide filter bandwidth reduces the energy jitters. Furthermore, if the bandwidth of filter is wide enough, the transmission rate and the reshape distance will make less effects on the variance of phonton number fluctuation.

Then we give the numerical results of the system on the modulator action. It is noticeable that the amplify space in the line affects energy jitters lightly. Only the high speed leads of the system to obvious energy jitters.

Comparing action between the filter and the modulator, we find that there exists a critical distance in this kind of soliton transmission. Over that point the variance of phonton number fluctuation increases rapidly.

In the earlier paper,[3] we learned that the variance of time fluctuation inverses to the filter bandwidth. How to solve this dilemma is the last problem we discuss in our paper. We derive the simplified expression of the energy jitters and the time jitters on the basis of engineer consideration, and work out how to choose the optimum system parameters of such soliton system, which may be useful for the design of the soliton transmission system.

1. J. P. Gordon, H. A. Haus, Optics Lett. **10**, 665 (1986).
2. L. F. Mollenauer, J. P. Gordon, S. G. Evangelides, Optics Lett. **17**, 1575 (1992).
3. A. Mecozzi, J. D. Moores, H. A. Haus, Y. Lai, J. Opt. Soc. Am. B **9**, 1350 (1992).

TuO4 **1430**

Semi-analytical method for performance analysis of soliton systems

J. R. F. da Rocha, L. B. Ribeiro, A. N. Pinto, *Dept. of Electronics & Telecommunications, University of Aveiro, 3800 Aveiro, Portugal*

Due to the combined effects of fiber nonlinearities, EDFA repeater noise, short pulse duration required for soliton systems and long-distance transmission, random phase fluctuations in the soliton carrier frequency lead to time jitter at the receiver side.[1,5] Combining the simulation of such a situation with a newly developed moment generating function (MGF) for the decision current, the bit-error rate of direct-detection receivers affected by signal jitter was estimated.

We consider a system with 5 transport sections separated by EDFA repeaters with optical power gain G and spontaneous emission factor n_{sp}. Each repeater has an output Fabry-Perot optical filter with equivalent bandwidth B_{eq}. Due to soliton interactions and Gordon-Haus effect, the incoming pulses suffer from time jitter. The electronic receiver, composed of a PIN detector, low-noise preamplifier, shaping filter, ideal clock extraction circuit[2] and a decision part, is considered in the MGF formulation.

The new formula copes with transmitter non-zero power extinction ratio, optical filtering, inter-symbol interference (ISI), arbitrary equalizer impulse response $h_r(t)$, and signal jitter due to nonlinear transmission. A sequence of information bits $\{a_k\}$ is transmitted using a train of pulses. At the receiver a stochastic deviation α_k, T affects each pulse k, with power envelope $h_p(t)$

$$p_{in}(\tau) = \sum_{k=-n}^{n} a_k \cdot h_p(\tau - kT - \alpha_k T) \quad (1)$$

As the $\{\alpha_k\}$ are mutually independent RV's, for a given realization of $\{\alpha_k\}$, the unconditioned MGF of the decision current at sampling instant, is related with the conditioned output Z' through $M_I(s) = E_{\{\alpha_k\}}[M_{Z'}(s, t_s)]$. Thus, the MGF for symbol i = a_0 is obtained by[3]

$$M_{I_i}(s) = \frac{E_{\alpha_0}[\exp\{a_0 B_0(\alpha_0,s,t_s)\}]}{A(s,t)} \cdot \prod_{\substack{k=-n \\ k\neq 0}}^{n} [I + E_{\alpha_k}[\exp\{B_k(\alpha_k,s,t_s)\}]] \quad (2)$$

where

$$A(s,t) = 2^{2n} \exp\left\{\int_{-\infty}^{\infty} B_{eq} \cdot \ln\left[1 - RN_0 \cdot \left(e^{sqh_r(t-\tau)} - 1\right)\right] d\tau\right\} \quad (3)$$

$$B_k(\alpha,s,t) = \int_{-\infty}^{\infty} \frac{R(e^{sqh_r(t-\tau)} - 1)}{1 - RN_0 \cdot (e^{sqh_r(t-\tau)} - 1)} \cdot h_p(\tau - kT - \alpha T) d\tau \quad (4)$$

R = $\eta\lambda/hc$ is the hole-electron pair generation rate, h is Planck constant, c is the speed of light in vacuum, η is the detector quantum efficiency and λ is the signal wavelength.

For low-jitter, a first order McLaurin expansion for $B_k(\alpha, \ldots)$ can be used, yielding

$$E_\alpha[\exp\{B_k(\alpha,s,t_s)\}] = \exp\{B_k(0,s,t_s)\} \cdot M_\alpha\left(\left.\frac{\partial B_k(\alpha,s,t_s)}{\partial\alpha}\right|_{\alpha=0}\right) \quad (5)$$

$M_a(s)$ is the MGF of the pulses stochastic arriving times. The required first derivative of B_k, is

$$\frac{\partial B_k(\alpha,s,t_s)}{\partial\alpha} = RGT \int_{-\infty}^{\infty} \frac{(e^{sqh_r(t_s-\tau)} - 1)h_p(\tau - kT - \alpha T)}{1 - RN_0(e^{sqh_r(t_s-\tau)} - 1)} d\tau \quad (6)$$

where $h_p'(t)$ represents the time derivative of the optical pulse $h_p(t)$. Taking into account the receiver thermal noise variance σ_{th}^2, the BER can be estimated via Chernoff bound, by minimizing (7) with respect to s[4]

$$BER < \exp\left(\frac{\sigma_{th}^2 \cdot s^2}{2}\right) \cdot \sqrt{M_{I_1}(-s) \cdot M_{I_0}(s)}, \qquad \forall s: s > 0 \quad (7)$$

The above formulations were used to study different aspects of the receiver. For the calculations we considered G = 2 dB = $\alpha L_{section}$. EDFA spontaneous emission factors n_{sp} of 20.6 and 50 were used. The receiver optical filter has B_{eq} = 167 GHz. PIN quantum efficiency is 1. $h_p(t)$ pulses with square hyperbolic secant shape were considered, having $T_0 = 8.33e^{-11}$ s leading to $L_D = L_{NL}$ = 347.2 km. Signal λ is 1550 nm, soliton peak power is 0.96 mW and the bit rate is swept from 0.7 to 1.1 Gbps.

The detected pulse eye-diagram can be viewed in Fig. 1.a and in Fig. 1.b the equalized current is shown for $1/T$ = 1 Gbps and n_{sp} = 20.6. The distribution of the arriving times is displayed in Fig. 2. A three quasi-Gaussian lobe characteristic is observed due to the dominance of neighbor bit interaction. $M_\alpha(s)$ is thus given by

$$M_\alpha(s) = A_- \exp\left(s\mu_{-1} + \frac{s^2 \cdot \sigma_{-1}^2}{2}\right) + A_0 \exp\left(s\mu_0 + \frac{s^2 \cdot \sigma_0^2}{2}\right) + A_{+1} \exp\left(s\mu_{+1} + \frac{s^2 \cdot \sigma_{+1}^2}{2}\right) \quad (8)$$

with the parameters A_x, μ_x and σ_x (with $x = i$ for bit a_i) being extracted from the histogram in Fig. 2. In Fig. 3 we apply the theory to estimate the signal jitter impact on the BER for very noisy EDFAs (high n_{sp}). The considered receiver includes a third order Butterworth shaping filter with f_c = 0.5 ($f_c = f_{3dB}T$). As can be

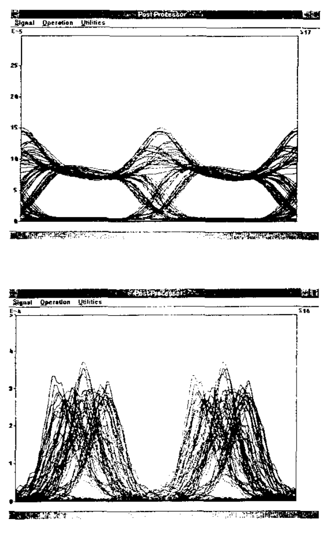

TuO4 Fig. 1. Eye-diagram of (a) solitons arriving at the detector and (b) equalized pulses simulated by SCORE.

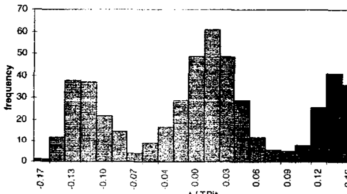

TuO4 Fig. 2. Distribution of incoming pulses average arriving time, affected by soliton interaction and Gordon-Haus effect.

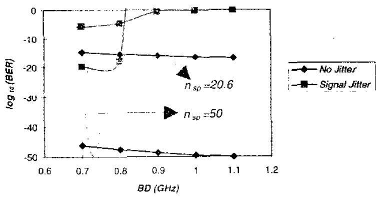

TuO4 Fig. 3. BER analytical estimates comparison with-without degradation due to signal jitter. The jitter statistics were estimated by simulation for n_{sp} = 20.6 and n_{sp} = 50.

seen for instance at $1/T$ = 1.1 Gbps, the BER degradation due to signal jitter can increase by a factor of $1e^{30}$ for n_{sp} = 50 and $1e^{10}$ for n_{sp} = 20.6.

In systems strongly submitted to noise and transmission non-linearity, the cumulative effects of clock jitter, soliton interaction and ISI can now be taken into account in a comprehensive analytical formulation. The advantage of this method over exhaustive Monte-Carlo simulations is the dramatic economy of computing time to calculate the BER.

1. D. Marcuse, "An Alternative Derivation of the Gordon-Haus Effect," IEEE Journal of Lightwave Tech. **10**, (2) 273–278, Feb/92.
2. L. B. Ribeiro, J. R. F. da Rocha, "Optically Preamplified Receivers Analysis including Sampling Jitter," CLEO'94—Anaheim-California (USA), 8–13 May 1994, Session CThI35.
3. L. F. B. Ribeiro, J. R. F. da Rocha, "Performance evaluation of EDFA preamplified receivers taking into account intersymbol interference," paper accepted by the 'Journal of Lightwave Technology.'
4. J. R. F. da Rocha, J. O'Reilly, "Linear Direct-Detection Fiber-Optic Receiver Optimization in the presence of Intersymbol Interference," IEEE Transactions on Communications, **COM-34**, (4), 365–374, April 1986.
5. T. Georges, F. Favre, "Influence of Soliton Interaction on Amplifier noise-induced Jitter: a first-order analytical solution," Optics Letters, **16** (21), 1656–1658, 1 November 1991.

TuO5 **1445**

Dispersion shifted fibers with low nonlinear sensitivity

N. Yamada, M. Sawada, A. Wada, K. Takahashi, R. Yamauchi, *Fujikura Ltd., 1440 Mutsuzaki, Sakura-shi, Chiba-ken, 285 Japan*

With the development of the high performance optical fiber amplifiers, long haul transmission systems such as submarine cable sytems have moved to non-regenerating one using the optical amplifiers. In the non-regenerating systems, accumulation of signal distortion caused by the fiber nonlinearity is one of the major problems, because optical signals travel thousands of kilometers without reshaping. Transmission fibers used in these systems should be redesigned after consideration on the nonlinear sensitivity. In this paper, we report design of dispersion shifted fibers with reduced optical nonlinearity.

Sensitivities for nonlinear effects such as SPM, XPM and FWM are determined by a ratio of the nonlinear refractive index n_2 and the effective cross section area A_{eff}. The smaller n_2 and the larger A_{eff}, the smaller nonlinear sensitivity. It is essential for reduction of n_2/A_{eff} to enlarge A_{eff}, because the n_2 of the dispersion shifted fiber is not largely dependent on its profile. As A_{eff} is nearly equal to $(\pi/4)$ MFD^2, enlargement of the MFD is substantially required.

The dual-shape-core (DSC) is one of the major index profiles for dispersion shifted fibers (DSF).[1,2] A large amount of DSC-DSF have been already installed in the field. A refractive index profile of DSC-DSF shown in Fig. 1 has more than two solutions satisfying zero dispersion at a certain wavelength when the core size is changed. Fig. 2 shows core radius dependencies of chromatic dispersion, mode field diameter and bending loss for uniform bending with a 20 mm diameter. A solution for a larger core radius (S. L. C) allows a smaller MFD and smaller bending loss while the solution for a

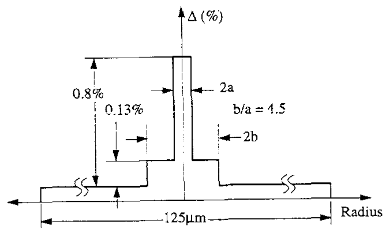

TuO5 Fig. 1. Refractive index profile of dual-shape-core dispersion shifted fiber.

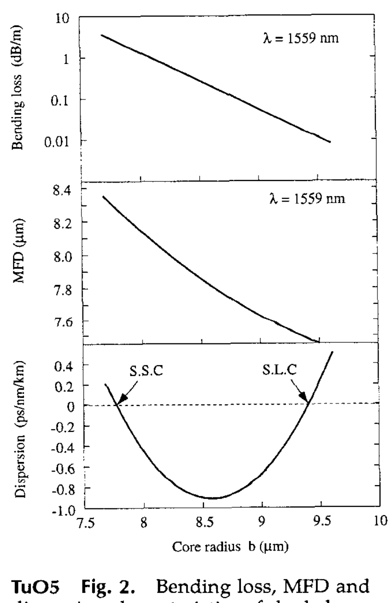

TuO5 Fig. 2. Bending loss, MFD and dispersion characteristics of dual-shape-core dispersion shifted fiber as a function of core diameter 2 b.

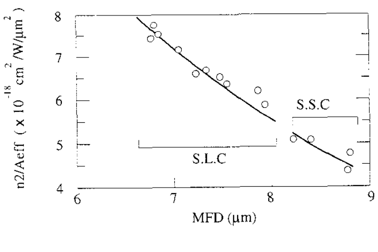

TuO5 Fig. 3. MFD dependence of n2/Aeff (circles : experimental data).

smaller core radius (S. S. C) leads to a larger MFD and larger bending loss. In the conventional design of DSC-DSF, the S. L. C. has been adopted in general because of its small bending loss performance. It, however, is possible to reduce n_2/A_{eff} by selecting the S. S. C although bending loss sensitivity increases to some extent. In actual design, the bending performance has been compromised with the mode field diameter (nonlinear sensitivity), the cutoff wavelength, the dispersion slope. As shown in Fig. 3, it is confirmed that the dual-shape-core dispersion shifted fibers with n_2/A_{eff} less than 5.5×10^{-18} cm^2/W/μm^2 can be realized with a bending loss less than 1 dB/m for uniform bending of 20 mm in diameter. This bending performance is sufficient for the practical cable design. The dispersion slope is a little increased to approximately 0.09 ps/km/nm^2.

The newly designed dispersion shifted fibers will be beneficial as long haul transmission fibers.

1. N. Kuwaki, M. Ohashi, C. Tanaka, N. Uesugi, Electron. Lett. **21**, 1186 (1986).
2. K. Nishide, D. Tanaka, M. Miyamoto, R. Yamauchi, K. Inada, OFC'88 (New Orleans, Louisiana), paper WI2.

TuP 1330–1500

Room 201B

Applications of Laser-Plasma X-Ray Sources

Yoshiro Owadano, Electrotechnical Laboratory, Japan, Presider

TuP1 (Invited) **1330**

Design and performance of a multi-hundred watt near diffraction limited diode pumped solid state laser for x-ray lithography applications

Lloyd Hackel, Mark Hermann, *Lawrence Livermore National Laboratory, University of California, Livermore, CA 94550*

We have developed and demonstrated a diode pumped solid state laser which produces 350 mJ per pulse in a 10 ns pulse length and currently runs at 650 Hz with near diffraction limited beam quality. The laser was primarily built to be a plasma driver producing x-rays at 130A for a projection lithography system. Numerous additional applications are antic-